ANALYTICAL MODEL FOR DYNAMIC AVALANCHE BREAKDOWN IN POWER DEVICES

L. Göhler, J. Sigg*

Universität der Bundeswehr München, Germany
*Siemens AG, Corporate Technology, Munich, Germany

Abstract. The behaviour of avalanche breakdown under the influence of initiating currents and generated carriers is analysed. It is shown, that these mechanisms cause a breakdown voltage shift and a self-limitating avalanche current. A GTO circuit model is enhanced by the findings and a circuit simulation with SABER demonstrates the gain in model accuracy.

Keywords. dynamic avalanche breakdown, avalanche breakdown, post-avalanche behaviour, safe operating area, turn-off failure, GTO turn-off

INTRODUCTION

The effect of impact ionization occurs in pn-junctions at high reverse voltages. In this case, carriers moving under the influence of the electric field from one end of the depletion region to the other get enough energy to ionize silicon atoms by impact. The generated electrons and holes contribute to the total current and can split other bonds if they get sufficiently accelerated, until the next impact happens. Impact ionization mainly takes place at the location of the maximum electric field. Consequently, there are, for instance, more free electrons than holes in the lightly doped n-region (ν-region) of a $p^+\nu$-junction and the net charge is reduced. According to Poisson's equation the electric field is not only determined by the ionized doping atoms, but also by the free charge carriers. Hence, the electric field has no longer a triangular shape, but is significantly lower over the increased width of the depletion region, just as shown by Wachutka [1]. This leads to a self-limitation of avalanche multiplication and therefore to a decrease of current slope with increasing reverse voltage (assumption of quasi-neutrality outside the depleted zone, Fig. 1). Avalanche current limitation appears either at high voltages and low initiating currents or at lower voltages and higher initiating currents (Fig. 2). Higher initiating currents, consisting of particles with the same charge as the ionized doping atoms in the lightly doped region, lead to a greater amount of generated charge carriers and therefore to a lower breakdown voltage. The shift of breakdown voltage is important when considering dynamic avalanche breakdown in power semiconductor devices.

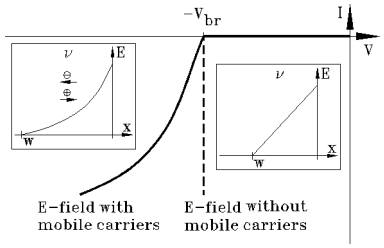

Fig. 1. Avalanche generation current in power devices *with* and *without* consideration of generated carriers (V_{br}: breakdown voltage).

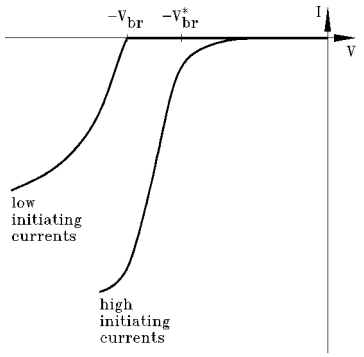

Fig. 2. Avalanche current for *low* and *high* initiating currents. Note the decrease of breakdown voltage and the different waveform at high currents (V_{br}, V^*_{br}: breakdown voltages).

THEORY

In this section approximations for the generated currents in $p^+\nu$- and $p^+\nu n^+$- structures under static conditions are derived. The first part focuses on the $p^+\nu$-structure (Fig. 3a; $N_\nu = N_d \ll N_{p^+}$). To ease calculation the coordinate system is moved, so that $E(x)$

equals zero at $x = 0$ ($w > 0$).

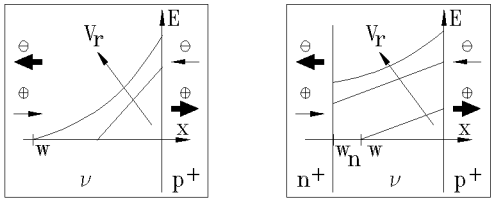

Fig. 3. Electric field in $p^+\nu$- (a) and $p^+\nu n^+$-structures (b) at various reverse voltages.

The basic equation describing impact ionization is Chynoweth's law [2], which can be combined with the static formulation of the continuity equation. G denotes the generation rate depending on the ionization rates of electrons (α_n) and holes (α_p) per unit length as well as the current density of each carrier type ($J_{n,p} \geq 0$).

$$G = \alpha_n \frac{J_n}{q} + \alpha_p \frac{J_p}{q} = \frac{1}{q}\frac{\partial J_p}{\partial x} + R \qquad (1)$$

$$\alpha_{n,p} = A_{n,p} \exp\left(-\frac{b_{n,p}}{E}\right)$$

($A_{n,p}$, $b_{n,p}$ = const.). At this point some assumptions are necessary to get an integrable form of (1):

- recombination can be neglected ($G \gg R$)
- the carrier velocity is constant and equal for electrons and holes:
  $v_n \approx v_p \approx v_s \approx 10^7 \frac{\mathrm{cm}}{\mathrm{s}}$
- instead of $\alpha_{n,p}$ an effective ionization rate α_i given by Ghandi [3] describes impact ionization and can be approximated according to Paul [4]:
  $\alpha_n \approx \alpha_p \approx \alpha_i = A_i \exp\left(-\frac{b_i}{E}\right)$,
  $\alpha_i \approx \alpha_0 \exp\left(m_1 E - m_2\right)$
  with [3]
  $A_i = 1.07 \cdot 10^6 \mathrm{cm}^{-1}$, $b_i = 1.65 \cdot 10^6 \frac{\mathrm{V}}{\mathrm{cm}}$,
  $\alpha_0 = A_i \exp\left(-\frac{b_i}{E_0}\right)$, $m_1 = \frac{b_i}{E_0^2}$, $m_2 = \frac{b_i}{E_0}$,
  $E_0 \approx 1.9 \cdot 10^5 \frac{\mathrm{V}}{\mathrm{cm}}$.

From Poisson's equation one gets ($J = J_n + J_p$):

$$E(x) = \int_{x'=0}^{x'=x} \left(\frac{2J_p}{\varepsilon v_s} + \frac{qN_d}{\varepsilon} - \frac{J}{\varepsilon v_s}\right) dx'. \qquad (2)$$

Inserting (2) into (1) leads to a second order differential equation and after some calculation to the desired value of J_{gen} (implicit function):

$$J_{gen} = J_p(w) - J_p(0) = J_p(w) - J_{p0},$$

$$J_{gen} = \frac{\sqrt{C_1}}{k_4} \coth\left(C_2\sqrt{C_1} - \frac{1}{2}\sqrt{C_1}w\right) - \frac{k_2}{k_4} - J_{p0} \qquad (3)$$

with

$$C_1 = \left(k_4 J_{p0} + k_2\right)^2 - 2k_5 \exp k_3,$$

$$C_2 = \frac{1}{\sqrt{C_1}} \mathrm{arcoth}\left(\frac{k_4 J_{p0} + k_2}{\sqrt{C_1}}\right)$$

and

$$k_1 = J\alpha_0, \quad k_2 = m_1\left(\frac{qN_d}{\varepsilon} - \frac{J}{\varepsilon v_s}\right), \quad k_3 = -m_2,$$

$$k_4 = \frac{2m_1}{\varepsilon v_s}, \quad k_5 = k_1 k_4.$$

The value of the total current density J at $x = w$ is:

$$J = J_0 + J_{gen} = J_{p0} + J_{n0} + J_{gen},$$

where J_{p0} and J_{n0} stand for the current densities, that initiate impact ionization, w represents the width of the depletion region and V_{jr} equals the sum of the reverse voltage and diffusion voltage. Neglecting the generated holes and assuming constant electron and hole currents over the whole depleted zone provides for the width w:

$$w \approx \sqrt{\frac{2V_{jr}}{\frac{qN_d}{\varepsilon} - \frac{J_{n0} - J_{p0} + J_{gen}}{\varepsilon v_s}}}. \qquad (4)$$

Eqn. (3) can be solved with a circuit simulator (for instance SABER). However, in consequence of the poor numerical stability this formula is not recommended for circuit models. A very brief expression requiring physical constants only follows from further simplification (generated holes neglected):

$$J_{gen} = \frac{m_0 J_0}{\frac{b_i}{2A_i V_{jr}} \exp\left(\frac{b_i}{\sqrt{2V_{jr}E'}}\right) - 1}, \qquad (5)$$

$$E' = \frac{qN_d}{\varepsilon} - \frac{J_{n0} - J_{p0}}{\varepsilon v_s} - \frac{J_{gen}}{m_0 \varepsilon v_s}. \qquad (6)$$

The factor m_0 was chosen for best agreement between (3) and (5):

$$m_0 \approx 1.35.$$

Eqn. (5) approximates (3) for an arbitrary ratio of J_{p0} and J_{n0} at low initiating currents and for $J_{p0} \gg J_{n0}$ at high initiating currents. These two cases are typically found in power semiconductor devices. Eqn. (5) can be implemented in circuit models easily.
Taking into account the temperature dependence of avalanche breakdown yields:

$$b_i(T) = b_{i0} + b_{i1}T + b_{i2}T^2,$$

$$A_i(T) = A_{i0} + A_{i1}T + A_{i2}T^2$$

and

$$v_s(T) = \frac{2.4 \cdot 10^7 \frac{\mathrm{cm}}{\mathrm{s}}}{1 + 0.8 \exp\left(\frac{T}{600\mathrm{K}}\right)}$$

($b_{in}, A_{in} = \mathrm{const.}$).

Now a $p^+\nu n^+$-configuration is considered. According to Fig. 3b this structure behaves equivalent to the $p^+\nu$-structure at low reverse voltages, i. e. the current slope is limited. In case of punch through, the width of the depletion region does not change. Electric field weakening has therefore less effect and the current can rise again rapidly at a certain value of reverse voltage ('second-step breakdown phenomenon', Takata et al. [5]). If the voltage drop over the n^+ - and p^+-region is sufficiently small one can derive for J_{gen}:

$$J_{gen} = \frac{m_0 J_0}{\frac{m_1 E'}{\alpha_0 \exp(m_1 E_n - m_2)(\exp(m_1 E' w^*) - 1)} - 1} \qquad (7)$$

($m_0 \approx 1.3$). E_n stands for the electric field at the border between the ν- and the n-region. With (4) (completed by m_0) the depletion region has a width of:

$$w^* = \begin{cases} w & : \quad w \le w_n \\ w_n & : \quad w > w_n \end{cases} . \qquad (8)$$

Definig now a variable E_n^* as:

$$E_n^* = \frac{V_{jr}}{w_n} - \frac{1}{2} E' w_n \qquad (9)$$

means for the value of E_n:

$$E_n = \begin{cases} 0 & : \quad E_n^* \le 0 \\ E_n^* & : \quad E_n^* > 0 \end{cases} . \qquad (10)$$

DYNAMIC AVALANCHE BREAKDOWN

The term dynamic avalanche breakdown describes an avalanche breakdown at high initiating currents ($J_{p0} \gg J_{n0}$) lowering breakdown voltage. These conditions exist in power devices only during switch-off, which explains the denotation 'dynamic'.

In principle, dynamic avalanche generation appears in various semiconductor power devices, but the amount of generated charge and consequently the influence on the voltage and current waveforms differs substantially. Normally, current densities in IGBTs, SCRs and diodes, for example, are too low for a significant breakdown voltage shift. GTOs, however, need a protection circuit to prevent demage.

When a GTO-thyristor is turned off, a large hole current flows out of the gate. Obviously, one part of the holes leaving the device moves through the reverse biased middle junction. If the voltage across the device rises too fast the middle junction breaks down far below the static breakdown voltage. The resulting high power loss destroys the device. In common applications the so-called snubber-capacity (C_{RCD} in Fig. 4) in parallel to the GTO limits the voltage slope during turn-off. Circuit simulation helps to find the appropriate value of C_{RCD} as an optimum between power loss, switching velocity and even the prevention of turn-off failures at the given voltage, current and temperature levels.

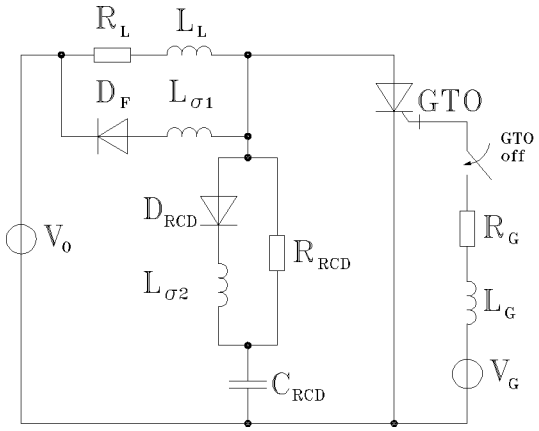

Fig. 4. DC-chopper ($V_0 = 4kV$, $V_G = -15V$, $R_L = 1.33\Omega$, $L_L = 25\mu H$, $R_{RCD} = 4\Omega$, $C_{RCD} = 6\mu F$, $R_G = 2m\Omega$, $L_G = 0.4\mu H$, $L_{\sigma 1} = L_{\sigma 2} = 0.2\mu H$).

The transient behaviour of avalanche generation needs further consideration. Assuming a constant anode-cathode voltage and a slight increase of hole current, for example, one can observe the following effects (Fig. 5). During a first (instable) phase of dynamic avalanche breakdown the additional holes lead to a higher slope of the electric field ($t = t_1$, Fig. 5), because it takes a certain time, until electrons and holes are generated by impact. After that neglectable short time span (first order estimation of duration: $t_2 - t_1 \approx \frac{2w}{v_s}$) quasi-static conditions predominate and

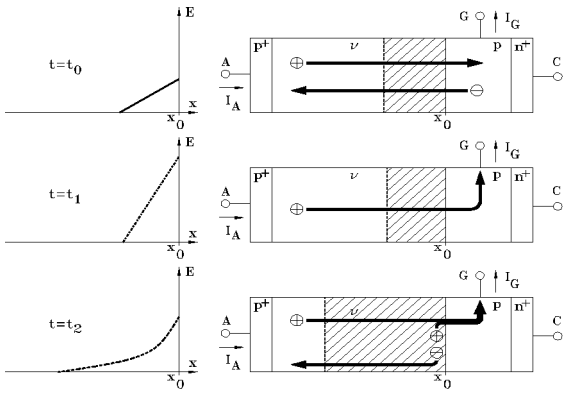

Fig. 5. Dynamic avalanche breakdown in a GTO, carrier flow and field distribution (t_0: before the onset of avalanche multiplication, t_1: instable case, t_2: stable case, i_a: anode current, i_g: gate current).

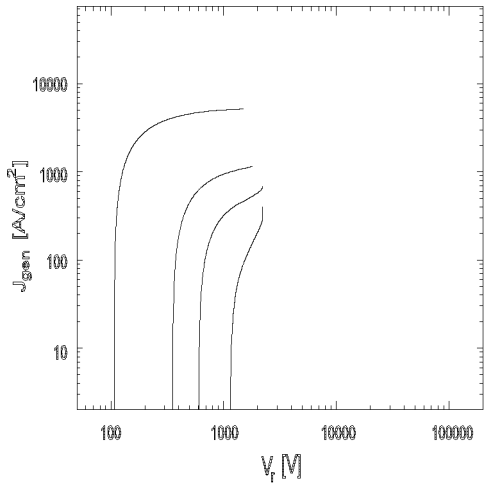

Fig. 6. Post-avalanche behaviour of $p^+\nu$-diodes, simulated with eqn. (7).

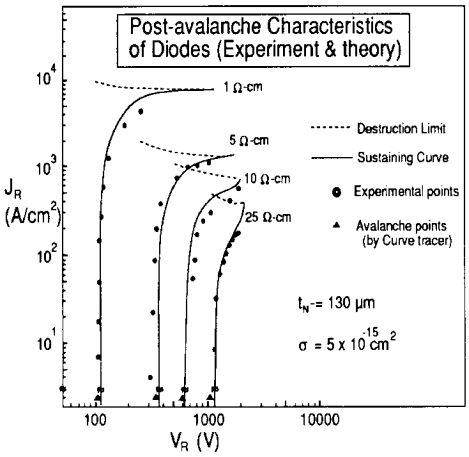

Fig. 7. Post-avalanche behaviour of $p^+\nu$-diodes, measured and numerically calculated with basic equations, taken from Takata et al. [5].

the findings outlined above are applicable ($t = t_2$, Fig. 5). Each time the voltage drop over the reverse biased middle junction or the initiating hole current changes its value the device goes through a similar cycle.

RESULTS

Avalanche generation at low initiating currents can be investigated by determining the v-i characteristic of $p^+\nu$-diodes for $V_{jr} > V_{br}$ (post-avalanche behaviour). Data published by Takata et al. [5] were used as a comparison. Fig. 6 displays the simulation, whereas Fig. 7 gives an impression of measurement ($w_\nu = 130\mu$m). The simulated curves are obtained from (7) and not from (5), because $p^+\nu$-diodes normally contain a thin n^+-layer, that lowers contact resistance. It can be seen, that both curves show good agreement.
Furthermore, the deviation of breakdown voltage calculated with (5) and (7) at low initiating currents to experimental results in Ghandi [3] does not exceed 10%

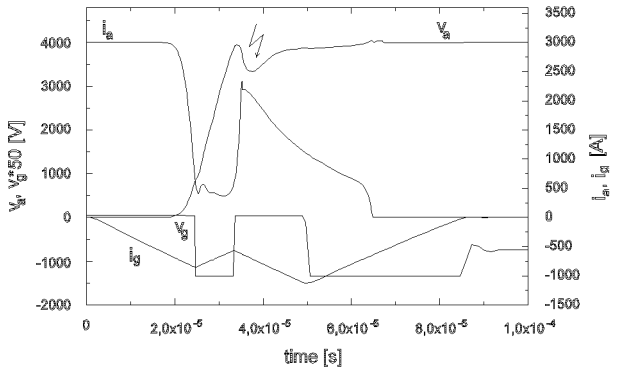

Fig. 8. Dynamic avalanche breakdown of a GTO-thyristor - circuit simulation with SABER. The flash symbol marks the point of maximum power dissipation (v_a: anode-cathode-voltage, v_g: gate voltage, i_a: anode current, i_g: gate current).

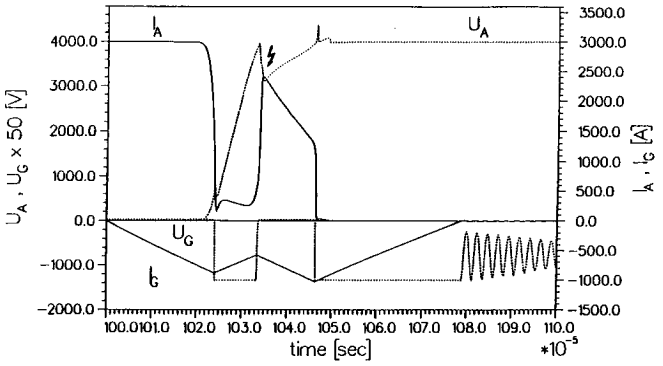

Fig. 9. Dynamic avalanche breakdown of a GTO-thyristor - 1-D device simulation with MEDUSA (taken from Gerstenmaier [6]). The flash symbol marks the point of maximum power dissipation (U_A: anode-cathode-voltage, U_G: gate voltage, I_A: anode current, I_G: gate current).

in the interesting range of doping.
The very fast destruction of a GTO-thyristor by dynamic avalanche breakdown makes it difficult to measure the needed current and voltage waveforms, but device simulation offers an acceptable benchmark substitute.
Fig. 8 and Fig. 9 show the device simulation by Gerstenmaier [6] and the circuit simulation with the improved GTO model based on Kraus [7] in SABER. In both cases the circuit equals that in Fig. 4.
The advantages of using (5) instead of a simple expression can be seen in an improved accuracy of the current-breakdown voltage characteristic at various current levels and a more gradual breakdown behaviour of the model, which is closer to reality.

CONCLUSION

An analytic description of dynamic avalanche breakdown phenomenon, suitable for circuit models has been presented. The solutions were applied to a quasi-

static description of dynamic avalanche breakdown, with the GTO-thyristor as an example. Comparisons with numerical simulations and measurements prove a good accuracy.

Acknowledgement

The authors wish to thank Prof. Hoffmann from Department of Electrical Engineering of University of Bundeswehr, Prof. Wachutka from Department of Physics of Munich University of Technology and Dr. Kögel from Department of Physics of University of Bundeswehr for their useful physical and mathematical hints.

Address of the Authors

Universität der Bundeswehr München
Werner-Heisenberg-Weg 39
D-85577 Neubiberg
Germany
Tel.: +49-89-6004-3665
Fax: +49-89-6004-2223
email: goehler@e4s21.et.unibw-muenchen.de

References

[1] G. K. Wachutka, Analytical Model for the Destruction Mechanism of GTO - Like Devices by Avalanche Injection, IEEE Trans. on El. Dev., vol. 38, No. 6, 1991, pp 1516-1523.

[2] A. G. Chynoweth, Ionization Rates for Electrons and Holes in Silicon, Physical Review 109, 1958, pp. 1537-1540.

[3] S. K. Ghandi, Semiconductor Power Devices, John Wiley & Sons, New York, 1977.

[4] R. Paul, Halbleiterelektronik, Dr. Alfred Hüthig Verlag, Heidelberg, 1975.

[5] I. Takata, T. Yamada, N. Soejima, Leakage Current and Breakdown Characteristics of P-N Diodes, Proc. of ISPSD '93, 1993, pp 205-211.

[6] Y. C. Gerstenmaier, 1-D Simulation and Analytic Theory of the Critical Turn-Off Behaviour of High-Power GTO-Thyristors with a Chopper Circuit, Proc. of ISPS '92, 1992.

[7] M. Bayer, R. Kraus, A new analytical GTO - Model for Circuit Applications, Proc. of PESC '95, 1995.